PHYSICAL REVIEW A VOLUME 18, NUMBER 5 NOVEMBER 1978

New interpretations, anomalous degeneracies, and SO(4) theory for electron correlation in first-row atoms and multiply-excited states

David R. Herrick and Michael E. Kellman
Chemistry Department and Institute of Theoretical Science, University of Oregon, Eugene, Oregon 97403
(Received 11 July 1978)

Geometrical and computational interpretations are offered for configuration-mixed $\alpha(1s^d 2s^2 2p^m) + \beta(1s^d 2p^{m+2})$ (where $d = 0$ or 2) valence states based on new profiles of L-shell mixing coefficients, correlation energies, and pair-function angular distributions for both ground and excited states. When viewed for species having the same degree of ionization Z-N, the profiles constructed for the internal and semi-internal "nondynamical" correlation energies computed by Sinanoğlu's "non-closed-shell many-electron theory" are found to display a striking, approximate particle-hole symmetry with respect to total L-shell occupancy. Near-degeneracy-type correlation energy for ^3P and ^1D levels of C-like atoms becomes exactly degenerate when the same radial functions are used for both states. The mixing structure for all L-shell states is described accurately by an N-electron operator $\Lambda(N) = \Sigma_{i<j}(A_i - A_j)^2$ with single-particle SO(4) generators A_i like the Runge-Lenz vector. $\Lambda(N)$ represents an approximate "correlation invariant" for L-shell mixings.

I. INTRODUCTION

Most atomic and molecular structure theory is explained first with a single configuration for states. Accurate energies and wave functions beyond Hartree-Fock (HF) for the states, however, require electron correlation effects due to Coulomb repulsions.[1] Although correlation describes a relatively small part of the total energy, it becomes crucial for explaining more sensitive probes of the many-electron wave function such as accurate radiative transition probabilities,[2] electron affinities,[3] bond energies,[4] hyperfine interactions,[5] photoionization and inner-shell processes including multiple excitations,[2(c),6-8] and scattering resonances,[9] to name just a few. Particularly strong correlations may prevail when near-degeneracy interactions occur for orbital configurations in either ground or excited states, causing a severe breakdown of the single-configuration classification for states. When this happens the usual perturbation approach becomes inadequate, and states must be classified more or less empirically by the relative signs and magnitudes of a few, dominant mixing coefficients in multiconfigurational states computed by direct energy matrix diagonalization. Near-degeneracy mixings have been described for molecular diatomic valence binding,[4] doubly excited atoms including electron affinities,[10] and excited states of polyenes,[11] illustrating only part of a more widespread and complicated phenomenon.

It would prove extremely useful for these problems to have at one's disposal an alternate method for generating the dominant configuration mixings of states, thereby avoiding the usual detailed, direct energy computation. Such a procedure might involve, say, an approximate "configuration-mixing invariant" constructed from Lie algebra generators for single-particle states taking into account physical attributes of only the *correlation* part of the problem, rather than total energies. In this way we would have a method for classifying the actual configuration-mixed states *beyond* the usual sets of quantum numbers provided by the exact symmetries for rotations, spin, parity, and molecular point groups. Even rough estimates of coefficients by this indirect method would be valuable for interpreting interference effects in computed transition matrix elements (propensity rules), or as a convenient starting point for more accurate energies by perturbation approaches.

Methods of this type involving SO(4) Lie algebras for atomic orbitals have already been described for two electrons in hydrogenic valence orbitals[10,12] and Rydberg configurations,[10,13] channel couplings occurring for actual He isoelectronic series including new SU(3)-type quantum numbers for radiative and autoionization transitions,[10,12(c),14] and very generally for angular correlations of an isolated atomic electron pair.[15] Some of the channel aspects[14] of these problems are analogous to the extremely useful angular momentum decoupling schemes for atom-diatom collisions,[16] and have brought substantial new order and insight to an otherwise complicated spectrum. Can similar methods be developed for many-electron (i.e., more than 2) systems? The present paper shows for the first time how to do this for the long-standing problem of $2s^2 2p^m - 2p^{m+2}$ near-degeneracy valence mixings for first row atoms and ions.

Along the way we uncover some fascinating new aspects of electron correlation including previously unnoticed accidental degeneracies for different states. The general nature of the physical origins for these new results may have strong implications for future classifications of correlation in atoms and molecules, as well as existing problems for nonergodicity[17] of correlations in classical systems.

Previous studies[18,19] of L-shell mixings by way of mathematically coupled SO(4) representations of states failed to identify the proper configuration mixings except by direct energy calculation. Here, we successfully describe accurate mixing coefficients for all L-shell states using a many-electron "correlation invariant" constructed with single-particle SO(4) generators in a pairwise fashion. In order to view the significance of this new result with a proper perspective we offer first, in Sec. II, a detailed numerical analysis of L-shell configuration mixing and correlation energies. In Sec. III we then explain these observed trends with more physical terms involving antisymmetry and coupled-pair function angular distributions. The group-theoretical description of states then follows in Sec. IV.

Near-degeneracy-type mixing of configurations $1s^2 2s^2 2p^m$ and $1s^2 2p^{m+2}$ is computationally well established.[20] The term "near-degeneracy" refers to an exact hydrogenic degeneracy of the two configurations in the nonrelativistic high-Z limit.[21] For all values of Z the $2s^2$-$2p^2$ correlation substantially improves the energy for the lower state. Sinanoğlu's "non-closed-shell many-electron theory" (NCMET) provides mathematically for distinguishing the different types of pair correlations in theoretical computations beyond HF.[1,22-26] The theory casts the exact nonrelativistic wave function and energy into a sum of terms

$$\Psi_{\mathrm{NR}} = \phi_{\mathrm{HF}} + \chi_{\mathrm{INT}} + \chi_F + \chi_U ,$$

and

$$E_{\mathrm{NR}} = E_{\mathrm{HF}} + E_{\mathrm{INT}} + E_F + E_U ,$$

representing separate contributions from HF plus "internal" plus "semi-internal" plus "external" pair correlations. Both E_{INT} and E_F are "nondynamical" in the sense that they display a strong state dependence with nuclear charge (Z) and number of electrons (N). E_U on the other hand is "dynamical," representing the short-range portion of the pair-interaction potential which changes slowly between different states. The near-degeneracy mixing constitutes the major portion of the internal correlation, and we use these terms interchangeably. Luken and Sinanoğlu[27] have provided tables of accurate nondynamical "charge" wave functions and energies of many L-shell states, based on restricted HF as the initial starting point.

In view of the rather extensive literature for the internal near-degeneracy correlation, what more remains to be explained? Our present analysis brings to light several new results and interpretations:

(i) Because $2s^2$-$2p^2$ correlation is nondynamical it has usually been described[20(b),24] for either fixed Z, fixed N, or for ground states on a state-by-state format. We construct new diagrams which show an overall configuration-mixing "profile" for all L-shell states having the same degree of ionization, $q \equiv Z - N$. With this new perspective we discover some interesting "accidental" degeneracies for different nondynamical correlation energies for iso-q species. Moreover, E_F and E_{INT} are found to display similar changes *between* states, indicating that these correlations may not be as independent as is generally thought. The results may have implications for a more general version of NCMET.[25] We show that E_{INT} has an exact degeneracy for ^3P and ^1D states of the C-like $1s^2 2s^2 2p^2$ configuration when the same restricted basis is used to describe both states. Splitting of this "correlation degeneracy" is found to be small for actual states, and originates with general considerations of antisymmetry and pairwise additive potential, rather than any specific details of Coulomb potentials.

(ii) New computations of similar profiles are made for internal correlation energies of doubly excited states, taking into account a Feshbach projection[28] for continuum stability. Multiply excited resonances are known for collisional excitations,[9(a)] beam-foil spectra,[29] and radiative double excitations at low Z.[9(a),30] Similar states would also occur for direct inner-shell ionization processes including possible simultaneous shake-up.[7,8] While accurate correlation energies are not yet available for multiply excited L-shell states, our present results show that the internal correlation may play a significant role for stability of anions.

(iii) Just as $2s$-$2p$ interaction accounts for simple molecular bond angles, $2s^2$-$2p^2$ mixing describes a relative angular (i.e., θ_{12}) hybridization for electron pair correlation in isolated atoms.[15] We construct a density function $\rho(\theta_{12})$ for pair correlation by first subtracting out "exclusion effects" due to antisymmetry exchange with other, noncorrelating electrons. The remaining distribution function shows that the two correlating electrons are squeezed closer together as additional valence electrons fill up the HF spin-

TABLE I. Term symbols and phase convention for $2s^2 2p^m$ and $2p^{m+2}$ states of the seven L-shell cases, neglecting the $(1s^2)^1S$ core. For notation, $(s\bar{s}01)$ represents a normalized Slater determinant for the product wave function $2s(\vec{r}_1)2s(\vec{r}_2)2p_0(\vec{r}_3)2p_1(\vec{r}_4)\alpha_1\beta_2\alpha_3\alpha_4$.

Case	m	Term	w	$2s^2 2p^m$	$2p^{m+2}$
1	0	^1S	3	$(s\bar{s})$	$\frac{1}{\sqrt{3}}[(-1\bar{1})-(0\bar{0})-(-\bar{1}1)]$
2	1	$^2P^0$	2	$(s\bar{s}1)$	$\frac{-1}{\sqrt{2}}[(-11\bar{1})+(0\bar{0}1)]$
3	2	^3P	1	$(s\bar{s}01)$	$(-101\bar{1})$
4	2	^1S	4	$\frac{1}{\sqrt{3}}[(s\bar{s}-1\bar{1})-(s\bar{s}0\bar{0})-(s\bar{s}-\bar{1}1)]$	$\frac{1}{\sqrt{3}}[(-\bar{1}0\bar{0}1)-(-10\bar{0}\bar{1})-(-1-\bar{1}1\bar{1})]$
5	2	^1D	1	$(s\bar{s}1\bar{1})$	$-(0\bar{0}1\bar{1})$
6	3	$^2P^0$	2	$\frac{1}{\sqrt{2}}[(s\bar{s}-11\bar{1})+(s\bar{s}0\bar{0}1)]$	$(-10\bar{0}1\bar{1})$
7	4	^1S	3	$\frac{1}{\sqrt{3}}[(s\bar{s}-\bar{1}0\bar{0}1)-(s\bar{s}-10\bar{0}\bar{1})-(s\bar{s}-1-\bar{1}1\bar{1})]$	$(-1-\bar{1}0\bar{0}1\bar{1})$

orbital sea. Further "geometrical" interpretations are provided by the SO(4) model in Sec. IV.

II. NUMERICAL ANALYSIS OF L-SHELL MIXINGS

A. 2×2 matrix representation

For each L, S symmetry the wave functions for $1s^d 2s^2 2p^m$ and $1s^d 2p^{m+2}$ are designated ϕ_A and ϕ_B, respectively. Only filled ($d=2$) or vacant ($d=0$) K shells will be considered. The near-degeneracy mixings are described by a mixed wave function

$$\phi = \alpha\phi_A + \beta\phi_B \tag{1}$$

with coefficients normalized by $\alpha^2+\beta^2=1$. Due to symmetry constraints only 7 out of 38 possible L-shell valence terms can exhibit this $2s^2$-$2p^2$ correlation. An important part of our analysis (Secs. III and IV) will be to derive the mixing coefficients α and β by methods avoiding direct energy computations. In order to compare these different approaches in a consistent fashion we herewith adopt the specific phase convention for states displayed in Table I. Energy matrix elements E_A, E_B, and E_{AB} have been described with the usual radial integrals[31] in several sources.[19,20(a),21] We can reexpress those results in a concise fashion here for the configuration mixings by means of the combinations

$$\begin{aligned} E_A+E_B =& 2I(2s)+2(m+1)I(2p)+F_0(2s,2s)+2mF_0(2s,2p)-mG_1(2s,2p)+(m^2+m+1)F_0(2p,2p) \\ &+\{10+10m-5m^2-3L(L+1)-12S(S+1)\}F_2(2p,2p)+d[2I(1s)+F_0(1s,1s)+2F_0(1s,2s) \\ &+2(m+1)F_0(1s,2p)-G_0(1s,2s)-(m+1)G_1(1s,2p)], \end{aligned} \tag{2}$$

and

$$\begin{aligned} E_A-E_B =& 2I(2s)-2I(2p)+F_0(2s,2s)+2mF_0(2s,2p)-mG_1(2s,2p)-(2m+1)F_0(2p,2p)+10(m-1)F_2(2p,2p) \\ &+d[2F_0(1s,2s)-G_0(1s,2s)-2F_0(1s,2p)+G_1(1s,2p)]. \end{aligned} \tag{3}$$

The terms in square brackets vanish when the K shell is empty. The off-diagonal energy is given by

$$E_{AB} = -\sqrt{w}G_1(2s,2p) \tag{4}$$

with appropriate values of w displayed in Table I.

Only the lower-energy state will be described for each case. Upper roots tend to interact with other excited states of the same symmetry, and are not well described by this approximation. The model yields the lower energy (E) directly as

$$2E = E_A+E_B-[(E_A-E_B)^2+4E_{AB}^2]^{1/2}, \tag{5}$$

depending generally on all three parameters E_{AB}, E_A+E_B, and E_A-E_B. The configuration mixing coefficients on the other hand are determined by

only two of the parameters in the ratio

$$\eta = (E_A - E_B)/2E_{AB}, \tag{6}$$

with η positive in our phase convention for states. Consequently α and β always have the same phase for the lower state, with their ratio given by

$$(\beta/\alpha) = -\eta + (1+\eta^2)^{1/2}. \tag{7}$$

The resulting configuration mixing is "weak" if $\eta \to \infty$, so that $\beta \to 0$. The strongest possible mixing for the lower state would occur when $\eta = 0$, in which case $\alpha = \beta$.

The near-degeneracy correlation energy contribution to $E_{\rm INT}$ is given generally as

$$E_{\rm INT} = E_{AB}(\beta/\alpha), \tag{8}$$

representing the energy lowering $E - E_A$ for the two-state model. Equation (8) continues to apply for wave functions containing additional configurations beyond ϕ_A and ϕ_B chosen according to NCMET constraints. The mixing ratio (β/α) does not change much when going from ϕ to a larger configuration basis. Valence states for all other L-shell terms not contained in Table I are described by single configurations, and therefore have $E_{\rm INT} \approx 0$. McKoy and Sinanoğlu[20(b)] have described $E_{\rm INT}$ for ground states. The present analysis will take a more general view of things, treating both ground states (cases 1–3) and excited states (cases 4–7) on the same footing for each degree of ionization q.

B. Filled K-shell states

Figure 1 shows the characteristic "profile" of the mixing coefficient α for $1s^2 2s^2 2p^m$ case by case across the first row. Here for neutrals cases 1–7 represent Be(^1S), B($^2P^o$), C(^3P), C(^1S), C(^1D), N($^2P^o$), and O(^1S), respectively. These values were computed from tables of configurational wave functions in Ref. 27. Other calculations[20] for various members of the profile yield similar values. The fairly sharp changes occurring for α between states illustrate the "nondynamical" aspect of internal correlation. The profile remains fairly stable with respect to degree of ionization, represented here by the notation A^q ($q = Z - N = -1, 0, 2, \ldots$). Values for finite $q > 0$ have been omitted from Fig. 1 for greater clarity, as they all lie between the curves for A and A^∞. At high Z, A^∞ describes mixings for the Coulomb repulsion operator

$$V = \sum_{i<j} \frac{1}{r_{ij}} \tag{9}$$

in a hydrogenic basis.[21] The mixings become stronger at low Z because of a larger $2s, 2p$ radial overlap for HF orbitals in comparison to hydrogenic overlap (cf. Sec. III). A stronger radial overlap enhances the possibility for angular correlation of electrons, thereby giving rise to more $2p^2$ character in the wave function.

Figure 2 shows the profiles of $E_{\rm INT}$ for anion, neutral, and positive ions. For consistency between different cases we have adapted all of these values from Ref. 27. For point of reference, the four values of $E_{\rm INT}$ at case 3 represent $(1s^2 2s^2 2p^2)^3P$ states of B^-, C, N^+ and O^{2+}. The nondynamical behavior of the correlation is clearly evident, although the overall shape of different profiles remains fairly stable with increasing values of Z. The hydrogenic theory[21] predicts a linear dependence for $E_{\rm INT}$ at high Z, with $-E_{\rm INT}/Z$ given by 0.32, 0.19, 0.08, 0.33, 0.08, 0.15, and 0.20 eV, respectively, for the cases 1–7.

C. Multiply excited states

Similar profiles are now computed for $2s^2 2p^m$ doubly excited configurations. Although energies

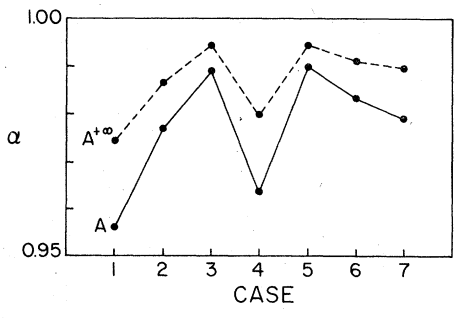

FIG. 1. Mixing profile for states $\alpha(1s^2 2s^2 2s^m) + \beta(1s^2 2p^{m+2})$. Values of α for neutrals (A) are adapted from NCMET charge-wave functions of Ref. 27. The hydrogenic limit ($A^{+\infty}$) is from Ref. 21(c). Table I and the text describe term symbols for cases.

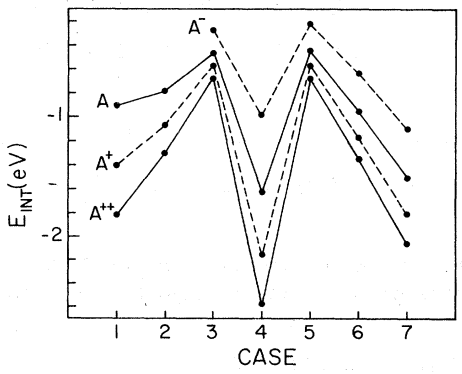

FIG. 2. Internal (near-degeneracy) correlation energy profiles for $1s^2 2s^2 2p^m$ iso-q species, $q \equiv Z - N$, constructed from NCMET energy tables of Ref. 27. High Z values are described in the text.

are available for many two- and three-electron species,[9(a)] there has been no systematic treatment of correlation energies of all the multiply excited L-shell states at a level comparable to the NCMET results for ground and valence excited states. This is partly due to the fact that cases 1–7 are now autoionizing resonances embedded in high-energy single- and double-ionization continua, and their computed wave functions suffer the usual stability problems. Chacon *et al.*[19] have computed hydrogenic Coulomb repulsion mixings, but that approach fails to recognize the different changes for $2s$ and $2p$ at low Z. Therefore, in order to provide better estimates of the near-degeneracy correlation we have determined anion, neutral, and singly charged states variationally. Values of the multiconfigurational energy E were optimized with a restricted radial basis including at first one STO($n=2$) per orbital. The internal correlation energy was then computed as the difference $E_{\rm INT}=E-E_A$. This value does not change significantly when E and E_A are optimized separately. In order to prevent a collapse of the $2s$ orbital exponent, and at the same time to effect an approximate Feshbach projection[28] against the single-ionization continuum, we Schmidt-orthogonalized the $2s$ orbital to an unscreened hydrogenic $1s$ orbital for each Z. This procedure gives an exact Feshbach projection for case 1 (i.e., $2s^2 \rightarrow 1s+e^-$), but it becomes more arbitrary for cases 2–7 in view of possible screening for the unoccupied $1s$ orbital. Values of the total energy are sensitive to this screening, and therefore have uncertain accuracy. $E_{\rm INT}$, however, is found to vary only several percent over large changes in $1s$ screening, and should provide more reasonable estimates for the internal correlation. Further refinement of the radial functions is not justified here.

The internal correlation is largely responsible for binding of the doubly excited $2s^2$ state of H^- relative to the threshold for $H(n=2)+e^-$ at 10.20 eV. A single configuration approximation for $2s^2$ gives 10.34 eV, just above threshold. The configuration-mixed state (ϕ) moves below threshold to 9.62 eV, closer to the experimental resonance[9(a)] at 9.56 eV (width = 0.04 eV). A third-order Z-expansion formula for the multiconfigurational Hartree-Fock energy[32] yields 9.84 eV. Most of the total correlation energy can be attributed to the $2s^2$-$2p^2$ interaction. Similar, strong mixing effects for two electrons are found for higher shells[10] where internal correlation dominates because of large separations between electrons. For He^- we find the $(2s^22p)^2P^o$ state at 58.2 eV, a full 1 eV above experiment and more accurate theory.[9(a),33] Part of this discrepancy is

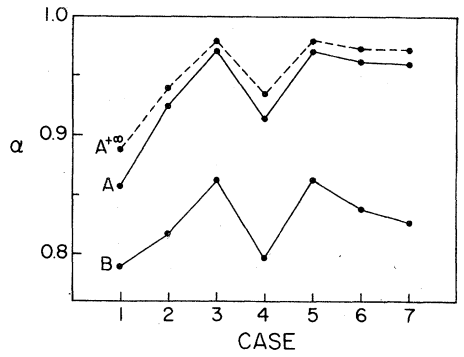

FIG. 3. Mixing profile computed for $\alpha(2s^22p^m)+\beta(2p^{m+2})$ doubly excited states for neutrals (A) and hydrogenic limit ($A^{+\infty}$). Curve B shows the Coulomb repulsion mixing profile when the same radial function is used for $2s$ and $2p$, illustrating strong radial overlap.

caused by our limited basis and the unscreened $1s$ orbital. To illustrate this effect more clearly, we note that our calculation becomes capable of reproducing the experimental value[9(a)] 57.2 eV if we use an effective $1s$ orbital exponent $Z'=1.5$ instead of the unscreened value $Z'=2$. However, our calculations for $E_{\rm INT}$ purposely omitted the other types of correlation, E_F and E_U, which become more important for anion binding as N increases.[3(b)]

Mixing profiles for α are displayed in Fig. 3. Those for $E_{\rm INT}$ are shown separately in Fig. 4. For reference, the anion profile reads $H^-(^1S)$, $He^-(^2P^o)$, $Li^-(^3P, ^1S, ^1D)$, $Be^-(^2P^o)$, and $B^-(^1S)$ from left to right. The effect of the empty K shell is to strengthen the $2s^2$-$2p^2$ correlation. This is illustrated by a stronger linear dependence for $E_{\rm INT}$ in the high-Z hydrogenic limit, where we find $-E_{\rm INT}/Z$ given by 0.75, 0.41, 0.17, 0.60, 0.17, 0.27, and 0.33 eV for cases 1–7, respectively.

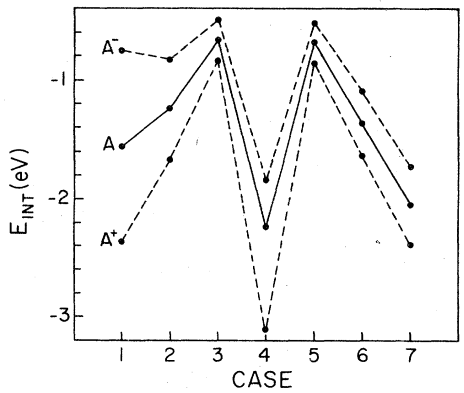

FIG. 4. Internal (near-degeneracy) correlation energy profiles computed for doubly excited $2s^22p^m$ states. High Z values are described in the text.

These values are roughly twice those appearing in Sec. II B for the filled K shell.

The hydrogenic Coulomb repulsion mixings once again have the largest values of α, coincident with their weak $2s$-$2p$ radial overlap. To see this effect more clearly we computed Coulomb repulsion mixings using a single unscreened Slater orbital for $2s$ and $2p$ with no $2s$-$1s$ orthogonalization, thus maximizing radial overlap to unity. This profile is shown near the bottom of Fig. 3, illustrating a strong mixing of states. When $2s$ is orthogonalized to $1s$ (e.g., hydrogenic $2s$) the curve shifts upward, and at the same time the $2s$-$2p$ radial overlap weakens.

D. Accidental correlation degeneracy

The shapes of the internal correlation energy profiles in Figs. 2 and 4 suggest an interesting approximate particle-hole type symmetry with respect to the number of electrons occupying L-shell orbitals. The nondynamical aspect of these profiles is strongest between cases 3–5 for ^3P, ^1S, and ^1D levels of the $2s^22p^2$ C-like valence configuration. Sinanoğlu[22(b)] has described the different correlation energies for these states. Here, we focus on a curious accidental near-degeneracy for $E_{\rm INT}$ (*not total energy*!) in the ^3P and ^1D levels, which has apparently gone unrecognized until now. The degeneracy grows stronger with increasing Z, eventually becoming *exact* in the hydrogenic limit. Both states have $L+S=2$.

The degeneracy has a relatively simple explanation with the two-state model in Sec. II A. Equations (6) and (8) show $E_{\rm INT}$ as a function of only two parameters, E_{AB} and E_A-E_B. Notice, however, that the difference E_A-E_B as described by Eq. (3) depends on only the state variable m, and not the values of L and S. Relative values of $E_{\rm INT}$ for C-like states are thus strongly controlled by E_{AB}, which turns out to be identical for ^3P and ^1D. Values of $E_{\rm INT}$ are therefore exactly degenerate when the *same* radial basis is used to describe both states, as illustrated by the hydrogenic limit. In actual atoms the radial functions become different for ^3P and ^1D, but the splitting introduced to the correlation degeneracy turns out to be small in a restricted orbital basis.

It is important to note that this degeneracy is a direct consequence of only three factors leading to the energy matrix elements: (i) pairwise additive potential, (ii) antisymmetry, and (iii) restricted $2s$, $2p$ spin-orbital basis. The precise form of the pair-interaction potential is unimportant here, except to determine splitting of the correlation energy. Whether these results can be explained by a higher symmetry classification of correlation beyond the usual atomic O(3)⊗SU(2) invariance for energies remains to be seen. In view of the approximate particle-hole symmetry for $E_{\rm INT}$, equivalent hybrid orbitals might provide a more reasonable starting point for describing the atomic correlation[15,34] in a restricted basis. A similar profile of NCMET correlations for higher shells[35] would also be helpful.

E. Semi-internal correlation

Whereas internal correlation describes the $2s^2$-$2p^2$ interaction, the remaining semi-internal part of the nondynamical correlation includes virtual pair transitions expelling one of the electrons out of the Hartree-Fock sea. Values of E_F are generally nonzero for open-shell states even when $E_{\rm INT}$ vanishes. For this reason the two types of nondynamical correlation are usually described separately.[24] Figure 5 shows a new profile for E_F constructed by the present approach. The results display three striking features: (a) the same approximate particle-hole symmetry continues to apply for E_F; (b) E_F varies in direct opposition to $E_{\rm INT}$ between neighboring cases; and (c) states having the same value of $L+S$ have nearly degenerate values for E_F. All values of energies have been adapted from the tables in Ref. 27. At first sight there seems to be no obvious explanation for the results based on the usual NCMET pair approach, since the total semi-internal energy represents a sum of several different pair energies.

Although $E_{\rm INT}$ and E_F tend[24] to decouple in computations, it may prove convenient to view the present results in the light of electrons correlating in the *coupled* state ϕ, rather than the single HF configuration ϕ_A. Are there, instead of the usual semi-internal correlation $\phi_{\rm HF}\rightarrow\chi_F$, modified virtual transitions of the type $\phi\rightarrow\chi_F$ taking into account a strong $2s^2$-$2p^2$ correlation at the outset?

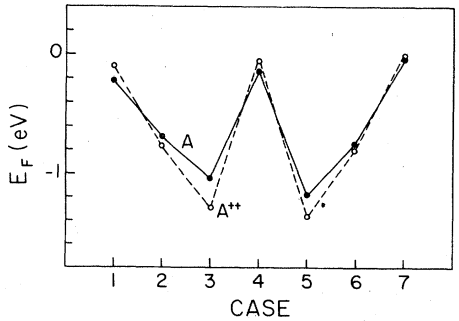

FIG. 5. Semi-internal correlation energy profiles for $1s^22s^22p^m$ states, constructed from NCMET energy tables of Ref. 27. For clarity only neutral (A) and doubly charged (A^{+2}) are shown.

In this way χ_F would directly reflect the overall mixing structure of ϕ, including antisymmetry exclusion effects (cf. Sec. III) and the corresponding L-shell mixing profiles. Silverstone and Sinanoğlu[25] have described a more general approach to NCMET along these lines. A detailed analysis of dipole transition moments for these states as to interference between different nondynamical contributions might show trends similar to those described here for $E_{\rm INT}$ and E_F.

III. GEOMETRY OF THE PAIR CORRELATION

Near-degeneracy correlation for first row ground states has been described with "exclusion" and "immersion" effects.[20(b)] Exclusion describes the decreasing availability of unfilled $2p$ orbitals for virtual $2s^2 - 2p^2$ transitions as additional electrons are added to the valence shell. Immersion describes changes in the correlation due to the variable HF potential for different states. We can show these effects separately for cases 1–7 by a representation of the state ϕ which is more consistent with the notion in Sec. II E for a strongly coupled pair. Rather than exclude possible configurations from $\chi_{\rm INT}$ initially[20(b)] we construct the L-shell mixings in the following way:

$$\phi = \hat{\mathfrak{a}}[\phi(12)u(3\cdots N)]. \tag{10}$$

Equation (10) contains three distinct parts: (i) an antisymmetrized ^1S pair wave function $\phi(12)$ describing $2s^2 \rightleftharpoons 2p^2$ mixing; (ii) an antisymmetrized wave function $u(3\cdots N)$ for additional electrons in $1s$ and $2p$ orbitals coupled for L, S symmetry; and (iii) the antisymmetrizer $\hat{\mathfrak{a}}$ for coupling of two electrons with $N-2$ electrons. Using the same notation for Slater determinants and spin orbitals from Table I, we can define the coupled-pair function generally by means of the mixing coefficient c in

$$\phi(12) = (s\bar{s}) + (c/\sqrt{3})[(-1\bar{1}) - (0\bar{0}) - (-\bar{1}1)]. \tag{11}$$

The remaining portion $u(3\cdots N)$ is then described by various single-configuration states in Table I including possible $1s^2$ occupancy. In this way the coupled wave functions for cases 2–7 may be viewed as resulting from successive coupling of independent $2p$ electrons to the pair of correlating electrons.

Exclusion effects occur when the factor $\hat{\mathfrak{a}}$ annihilates terms in the product function $\phi(12)u(3\cdots N)$ having two electrons in the same spin orbital. This affects only the $2p^2$ portion of $\phi(12)$, causing a renormalization of the mixing ratio to

$$(\beta/\alpha) = c(w/3)^{1/2} \tag{12}$$

TABLE II. Mixing coefficients for low-energy states $\alpha(2s^2 2p^m) + \beta(2p^{m+2})$ predicted by a "rigid" pair correlation function with $c = 1/\sqrt{3}$ in Eqs. (10)–(12).

Case	Term	α	β
1	^1S	0.8660	0.5000
2	$^2P^0$	0.9045	0.4264
3	^3P	0.9487	0.3162
4	^1S	0.8321	0.5547
5	^1D	0.9487	0.3162
6	$^2P^0$	0.9045	0.4264
7	^1S	0.8660	0.5000

for values of w in Table I. To see this effect, Table II shows mixing coefficients computed with the same pair function $\phi(12)$ for all seven cases. This model supposes (incorrectly!) a "rigid" pair correlation independent of all other electrons except by antisymmetry. The single value $c = 1/\sqrt{3}$ used here describes an ideal angular pair correlation hybridization.[15] The method reproduces the correct signs for α and β, as well as some of the oscillations in Figs. 1 and 3.

Immersion effects cause the actual pair function $\phi(12)$ to flex slightly from state to state as more electrons are added. They appear in the energy matrix elements via the difference $E_B - E_A$, representing a promotion energy for the $2s^2 \rightarrow 2p^2$ transition in the many-electron environment. From Eq. (3) we see that this energy increases linearly with valence-shell occupation, thereby weakening the overall mixing. The combination of these effects produces the characteristic profiles in Figs. 1 and 3. In order to see the effects of immersion separately, we have computed values of c in Eq. (12) which reproduce the exact values of (β/α)

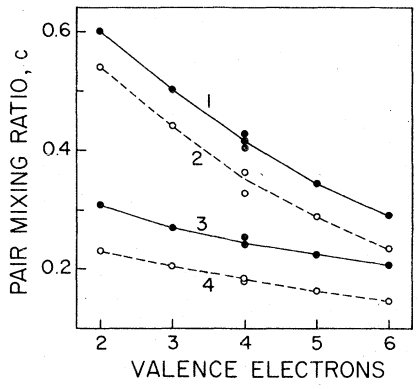

FIG. 6. Pair-function mixing-ratio coefficient c for Eq. (11), fitted to the many-electron mixings of Figs. 1 and 3. Here curves are labeled $1(2s^2 2p^m$, neutral), $2(2s^2 2p^m$, hydrogenic), $3(1s^2 2s^2 2p^m$, neutral), and $4(1s^2 2s^2 2p^m$, hydrogenic).

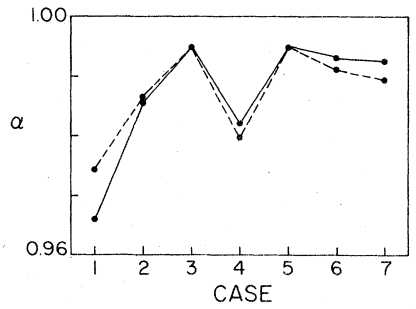

FIG. 7. Mixing profile for states $\alpha(1s^2 2s^2 2p^m) + \beta(1s^2 2p^{m+2})$ computed with new SO(4) operator $\Lambda(N)$ shown as (——), compared to hydrogenic Coulomb mixings (----).

for states in Sec. II. Values for neutrals and the hydrogenic limit for both filled and empty K shells are shown together in Fig. 6. As expected these mixings weaken as additional electrons cluster around the correlating pair.

The values for c determine much of the geometry of the spherical pair correlation distribution along the coordinates r_1, r_2, and θ_{12}. Geometries of this type are known for isolated pairs.[15,36] Here we consider the average angular distribution $\rho(\theta_{12})d\theta_{12}$ defined by integrating $|\phi(12)|^2$ over all spin and space coordinates for 1 and 2 except the interelectron angle θ_{12}:

$$\rho(\theta_{12}) = \rho_0 \sin\theta_{12}(1 - 2XS^2 + X^2), \tag{13}$$

with

$$X = c\sqrt{3}\cos\theta_{12},$$

and radial overlap

$$S = \int_0^\infty R_{2s}(r)R_{2p}(r)r^2\,dr. \tag{14}$$

The constant $\rho_0 = 1/(2 + 2c^2)$ is chosen for normalization

$$\int_0^\pi \rho(\theta_{12})d\theta_{12} = 1. \tag{15}$$

The restricted HF orbitals of Ref. 27 give $S \sim 0.95$ for neutrals. This value decreases slowly for higher Z, eventually approaching the exact hydrogenic value $S = \sqrt{3}/2 \sim 0.86$. Our doubly excited functions yield a similar trend, starting with $S \sim 0.95$ for anions and approaching the same hydrogenic limit. The angular distribution peaks at $\theta = 90°$ when $c = 0$ for uncorrelated $2s$ electrons. The peak moves to higher angles for physical states $c > 0$, due to pair hybridization by $\cos\theta_{12}$. The maximum densities for two valence electrons (i.e., case 1) occur at the following angles $\theta_{12}^{\max}$: 133°(He, empty K shell), 130°(hydrogenic, empty K shell), 123°(Be, filled K shell), and 117° (hydrogenic, filled K shell). These values for $\theta_{12}^{\max}$ decrease approximately 2°–3° for each extra electron added to the valence shell, with the largest changes occurring for the doubly excited states. Overall these results indicate additional "squeezing" of the correlating electron pair as the HF sea fills up around it.

IV. COMPARISON WITH MIXINGS PREDICTED BY AN SO(4) CORRELATION INVARIANT

Since much of the nondynamical behavior of the L-shell correlation is apparently controlled by factors (i.e., antisymmetry and number of valence electrons) other than the explicit form of the Coulomb potential itself, it is reasonable to expect similar mixing trends for other pairwise interactions. We now show that one such operator constructed from SO(4) Lie algebra generators of single-particle states gives an excellent approximation to the actual L-shell mixings, thereby providing a new geometrical interpretation of states.

A. Single-particle states

The SO(4) Lie algebra is defined here for the usual single-particle states $|nlm\rangle$ by the orbital angular momentum $\vec{L}$ and a vector $\vec{A}$ which satisfy

$$\begin{aligned} &[L_j, L_k] = i\epsilon_{jkm}L_m, [L_j, A_k] = i\epsilon_{jkm}A_m, \\ &[A_j, A_k] = i\epsilon_{jkm}L_m. \end{aligned} \tag{16}$$

The Casimir invariants on this basis are given by $L^2 + A^2 = n^2 - 1$ and $(\vec{L}\cdot\vec{A}) = 0$. We adhere to previous[14,15] phase conventions for generators and states, with $\vec{A}$ defined by

$$\begin{aligned} &A_0|1s\rangle = 0 \\ &A_0|2s\rangle = |2p_0\rangle, \quad A_0|2p_0\rangle = |2s\rangle, \\ &A_0|2p_{\pm 1}\rangle = 0. \end{aligned} \tag{17}$$

The Runge-Lenz operator provides a concrete representation for $\vec{A}$ in a hydrogenic basis, characteristic of the Lie algebra for rotations on a four-dimensional hypersphere in momentum space.[37] Here we can represent $\vec{A}$ in a form

$$\vec{A} = n(\vec{p}Q - \vec{r}P), \tag{18}$$

similar to a generalized angular momentum. Now, however, Q is the infinitesimal generator for scale transformations,

$$Q = (\vec{r}\cdot\vec{p}), \tag{19}$$

while P denotes a conjugate "momentum"

$$P = -i[Q, H] \tag{20}$$

$$= p^2 - 1/r \tag{21}$$

for the hydrogen atom energy (atomic units)

$$H=\tfrac{1}{2}p^2-1/r. \tag{22}$$

Average values of P vanish for hydrogenic states on account of the well-known virial theorem for scaling.[38] Geometrical characteristics of the hydrogenic SO(4) generator $\vec{A}$ are evident in the following operator replacements (for constant n only):

$$\vec{r}=\tfrac{3}{2}n\vec{A}, \tag{23}$$

$$\hat{r}=(1/n)\vec{A}, \tag{24}$$

$$r=(1/2)(2n^2+1+A^2), \tag{25}$$

$$r^2=(n^2/2)(2n^2+4+3A^2). \tag{26}$$

B. Many-electron states

The exact nonrelativistic N-electron states have spin and total angular momentum $(\vec{L}_1+\vec{L}_2+\cdots+\vec{L}_n)^2=L(L+L)$ conserved. The usual single-configuration states have the commuting one-electron operators

$$\sum_i L_i^2,\quad \sum_i A_i^2$$

diagonal. In order to describe configuration mixings between different states having the same quantum numbers L, S, and parity, we introduce coupling between single-particle states having different values of l. Whereas the exact energy involves an infinite tensor expansion of the Coulomb repulsion, valence states for two electrons are found to be well represented by the eigenstates of the simple operator $(\vec{A}_1-\vec{A}_2)^2$ over a wide range of values for n and L.[12,15] States having larger values of $(\vec{A}_1-\vec{A}_2)^2$ offer a more favorable spatial correlation for the electrons.[12(a),15,36] Our analysis in Sec. III suggests that similar results should hold for N electrons, with differences in the pair correlation resulting mainly from the effects of antisymmetry for additional, noncorrelating electrons. We therefore construct the operator

$$\Lambda(N)=\sum_{i<j}(\vec{A}_i-\vec{A}_j)^2 \tag{27}$$

representing a pairwise additive "harmonic" interaction between SO(4) generators for different electrons.

$\Lambda(N)$ as defined in Eq. (27) is not a many-electron invariant in the usual mathematical sense for Lie algebras. Previous studies[18] of L-shell mixings have looked into the possibility[39] that such mathematically coupled states for a diagonal Lie algebra Casimir invariant might somehow give the correct many-electron mixings. They didn't.[19]

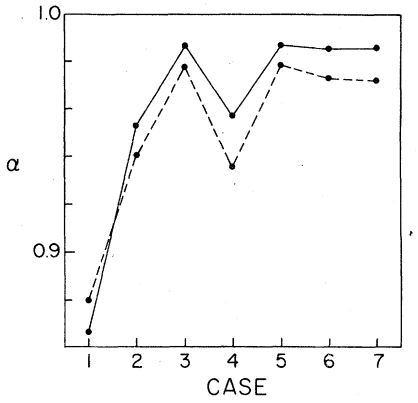

FIG. 8. Mixing profile for states $\alpha(2s^2 2p^m)+\beta(2p^{m+2})$ computed with new SO(4) operator $\Lambda(N)$ shown as (——), compared to hydrogenic Coulomb mixings (----).

In contrast, we find here that eigenstates of $\Lambda(N)$ are considerably more physical. Profiles of mixings computed with $\Lambda(N)$ are displayed in Figs. 7 and 8 for comparison with the corresponding hydrogenic Coulomb repulsion profiles. The close agreement is striking, and shows that $\Lambda(N)$ indeed represents an approximate, L-shell correlation invariant. At first sight the different mixing profiles for filled and unfilled K shell states might seem puzzling, since the SO(4) generators in Eq. (17) do not connect states in different shells. In order to explain this behavior, we expand Eq. (27) to

$$\Lambda(N)=(N-1)\sum_i A_i^2-2\sum_{i<j}\vec{A}_i\cdot\vec{A}_j. \tag{28}$$

The first term is diagonal in the configuration basis, and scales linearly as the number of electrons increases. The second term, however, describes the $2s^2$-$2p^2$ interaction and has the same matrix elements whether the K shell is filled or not. The configuration mixings therefore tend to become stronger as the K-shell electrons are removed. The method also describes an exact correlation degeneracy of $\Lambda(N)$ for cases 3 and 5.

The simple 2×2 matrix representation of L-shell correlation makes it possible to describe the exact mixing structure for each of the seven cases by fitting a single parameter γ in the following generalized version of $\Lambda(N)$:

$$\Lambda_\gamma=\gamma\sum_i A_i^2-2\sum_{i<j}\vec{A}_i\cdot\vec{A}_j. \tag{29}$$

The corresponding configuration mixing parameter for matrix elements of Λ_γ is $\eta=\gamma/\sqrt{w}$, from which values of γ for each case are extracted using η in Eq. (6). In this way we find that the hydrogenic

Coulomb repulsion mixings for the entire L shell can be described with a single formula

$$\gamma = \tfrac{17}{30} N \tag{30}$$

for doubly excited states ($N = m + 2$), or alternatively

$$\gamma = \tfrac{17}{30}(N + 2.260) \tag{31}$$

when the K shell is filled ($N = m + 4$).

In a similar fashion we can evaluate γ for a pure harmonic oscillator potential between electrons. By Eqs. (23) and (26) we find that for N electrons in the *same* shell the potential becomes

$$V_{\mathrm{HO}} = \sum_{i<j} (\vec{r}_i - \vec{r}_j)^2 = N(N-1)n^2(n^2+2) + (\tfrac{3}{2}n)^2 \Lambda_\gamma , \tag{32}$$

with $\gamma = \frac{2}{3}(N-1)$ for all values of n. When $n = 2$ the harmonic oscillator potential predicts slightly stronger configuration mixings than $\Lambda(N)$, with values of α 2%–5% lower than those in Fig. 8 for doubly excited states.

V. CONCLUDING REMARKS

New questions and interpretations for electron correlation have been brought to light, based on available theoretical values for nondynamical correlation energies for first row atoms. The present SO(4) model potential adequately describes these mixings. A more general group theory for correlation designed along the lines of NCMET would hopefully elucidate a possible higher symmetry for most of the nondynamical part of the fluctuation potential in a restricted HF sea plus finite semi-internal basis. Similar studies of this type for higher shells and molecular π structures would offer additional insight to underlying principles governing configuration mixing phenomena and pair interactions.

ACKNOWLEDGMENTS

This work was supported by NSF Grant No. CHE-76-10332. Acknowledgment for partial support is made to the Donors of the Petroleum Research Fund, administered by the American Chemical Society.

[1] For an account of electron correlation including much historical background see O. Sinanoğlu and K. A. Brueckner, *Three Approaches to Electron Correlation in Atoms* (Yale, New Haven, 1970).

[2] (a) P. Westhaus and O. Sinanoğlu, Phys. Rev. 183, 56 (1969). (b) A. W. Weiss, Phys. Rev. 162, 374 (1967). (c) J. W. Cooper, U. Fano, and F. Prats, Phys. Rev. Lett. 10, 518 (1963).

[3] (a) H. Hotop and W. C. Lineberger, J. Phys. Chem. Ref. Data 4, 540 (1975). (b) I. Öksüz and O. Sinanoğlu, Phys. Rev. 181, 54 (1969).

[4] (a) G. Das and A. C. Wahl, J. Chem. Phys. 56, 1769 (1972). (b) P. A. Benioff, G. Das, and A. C. Wahl, J. Chem. Phys. 67, 2449 (1977).

[5] O. Sinanoğlu and D. R. Beck, Chem. Phys. Lett. 20, 221 (1973); 21, 247 (1973).

[6] (a) S. Süzer, S.-T. Lee, and D. A. Shirley, Phys. Rev. A 13, 1842 (1976). (b) J. E. Hansen, Phys. Rev. A 15, 810 (1977).

[7] *Atomic Inner-Shell Processes*, edited by B. Crasemann (Academic, New York, 1975), Vol. 1.

[8] *Photoionization and Other Probes of Many-Electron Interactions*, edited by F. J. Wuilleumier (Plenum, New York, 1975).

[9] (a) G. J. Schulz, Rev. Mod. Phys. 45, 378 (1973). (b) M. J. Seaton, Proc. Phys. Soc. London 77, 174 (1961).

[10] D. R. Herrick and O. Sinanoğlu, Phys. Rev. A 11, 97 (1975).

[11] I. Ohmine, M. Karplus, and K. Schulten, J. Chem. Phys. 68, 2298 (1978).

[12] (a) O. Sinanoğlu and D. R. Herrick, J. Chem. Phys. 62, 886 (1975); Chem. Phys. Lett. 31, 373 (1975). (b) C. Wulfman, Chem. Phys. Lett. 23, 370 (1973). (c) D. R. Herrick, J. Math. Phys. 16, 1047 (1975).

[13] (a) S. I. Nikitin and V. N. Ostrovsky, J. Phys. B 9, 3141 (1976). (b) S. I. Nikitin, Opt. Spectrosc. (USSR) 42, 459 (1977).

[14] (a) D. R. Herrick, Phys. Rev. A 12, 413 (1975). (b) D. R. Herrick, Phys. Rev. A 17, 1 (1978).

[15] (a) D. R. Herrick, J. Chem. Phys. 67, 5406 (1977). (b) D. R. Herrick (unpublished).

[16] (a) P. McGuire and D. J. Kouri, J. Chem. Phys. 60, 2488 (1974). (b) D. J. Kouri, T. G. Heil, and Y. Shimoni, J. Chem. Phys. 65, 226 (1976); 65, 1462 (1976).

[17] (a) J. Moser, *Stable and Random Motions of Dynamical Systems* (Princeton University, Princeton, N. J., 1973). (b) D. W. Noid and R. A. Marcus, J. Chem. Phys. 62, 2119 (1975).

[18] (a) J. Alper and O. Sinanoğlu, Phys. Rev. 177, 77 (1969). (b) J. Alper, Phys. Rev. 177, 86 (1969). (c) C. Wulfman, Phys. Lett. A 26, 397 (1968).

[19] E. Chacon, M. Moshinsky, O. Novaro, and C. Wulfman, Phys. Rev. A 3, 166 (1971).

[20] (a) D. R. Hartree, W. Hartree, and B. Swirles, Philos. Trans. R. Soc. London Ser. A 238, 229 (1939). (b) V. McKoy and O. Sinanoğlu, J. Chem. Phys. 41, 2689 (1964). (c) E. Clementi and A. Veillard, J. Chem. Phys. 44, 3050 (1966). (d) P. S. Bagus and C. M. Moser, Phys. Rev. 167, 13 (1968). (e) J. Hinze and C. C. J. Roothaan, Prog. Theor. Phys. (Kyoto) 40, 37 (1967). (f) N. Sabelli and J. Hinze, J. Chem. Phys. 50, 684 (1969). (g) A. P. Jucys, Adv. Chem. Phys. XIV, 191 (1969). (h) O. Sinanoğlu, Adv. Chem. Phys. XIV, 237 (1969).

[21] (a) D. Layzer, Ann. Phys. (N.Y.) 8, 271 (1959). (b) J. Linderberg and H. Schull, J. Mol. Spectrosc. 5, 1 (1960). (c) M. Cohen and A. Dalgarno, J. Mol.

Spectrosc. 10, 378 (1963).
[22](a) O. Sinanoğlu, in *Atomic Physics*, edited by B. Bederson *et al.* (Plenum, New York, 1969), Vol. II. For earlier versions of the theory (MET), see also Ref. 1. (b) O. Sinanoğlu, Comments At. Mol. Phys. 1, 116 (1969).
[23]O. Sinanoğlu and I. Öksüz, Phys. Rev. Lett. 21, 507 (1968).
[24]I. Öksüz and O. Sinanoğlu, Phys. Rev. 181, 42 (1969).
[25]H. J. Silverstone and O. Sinanoğlu, J. Chem. Phys. 44, 1899, 3608 (1966).
[26]O. Sinanoğlu and B. J. Skutnik, J. Chem. Phys. 61, 3670 (1974).
[27]W. L. Luken and O. Sinanoğlu, At. Data Nucl. Data Tables 18, 525 (1976).
[28]H. Feshbach, Ann. Phys. (N.Y.) 19, 287 (1962).
[29](a) *Beam-Foil Spectroscopy*, edited by I. A. Sellin and D. J. Pegg (Plenum, New York, 1976). (b) *Topics in Current Physics*, Vol. 1, edited by S. Bashkin (Springer-Verlag, Berlin, 1976).
[30]R. P. Madden and K. Codling, Astrophys. J. 141, 364 (1965).
[31]E. U. Condon and G. H. Shortley, *Theory of Atomic Spectra* (Cambridge University, Cambridge, England, 1967).
[32]C. S. Sharma and R. G. Wilson, J. Phys. B 3, 1279 (1970).
[33](a) M. Ahmed and L. Lipsky, Phys. Rev. A 12, 1176 (1975). (b) C. A. Nicolaides and D. R. Beck, J. Chem. Phys. 66, 1982 (1977).
[34]O. Sinanoğlu and B. Skutnik, Chem. Phys. Lett. 1, 699 (1968).
[35](a) J. S. Alper, B. J. Skutnik, and M. Wilson, J. Chem. Phys. 56, 2402 (1972). (b) V. McKoy and O. Sinanoğlu, in *Modern Quantum Chemistry*, edited by O. Sinanoğlu (Academic, New York, 1962), Vol. 2, p. 23.
[36]P. Rehmus, M. E. Kellman, and R. S. Berry, Chem. Phys. 31, 239 (1978).
[37](a) V. Bargmann, Z. Phys. 99, 576 (1936). (b) Additional literature for hydrogenic SO(4) is too extensive for adequate treatment here. See M. J. Englefield, *Group Theory and the Coulomb Problem* (Wiley, New York, 1972).
[38]P.-O. Löwdin, J. Mol. Spectrosc. 3, 46 (1959).
[39]M. Moshinsky, Phys. Rev. 126, 1880 (1962).